Available online at www.sciencedirect.com
ScienceDirect
Biochimica et Biophysica Acta 1773 (2007) 615–630
Biochimica et Biophysica Acta BBA
www.elsevier.com/locate/bbamcr

Review

Myosin at work: Motor adaptations for a variety of cellular functions

Christopher B. O'Connell [a], Matthew J. Tyska [b], Mark S. Mooseker [a,c,d,*]

[a] Department of Cell Biology, Yale University School of Medicine, New Haven, CT 06511, USA
[b] Department of Cell and Developmental Biology, Vanderbilt University Medical Center, Nashville, TN 37232, USA
[c] Department of Molecular, Cellular and Developmental Biology, KBT 352, Yale University, PO Box 208103, New Haven, CT 06520-8103, USA
[d] Department of Pathology, Yale University School of Medicine, New Haven, CT 06511, USA

Received 28 February 2006; received in revised form 22 May 2006; accepted 30 June 2006
Available online 8 July 2006

Abstract

Cells have evolved multiple mechanisms to overcome the effects of entropy and diffusion to create a highly ordered environment. For cells to function properly, some components must be anchored to provide a framework or structure. Others must be rapidly transported over long distances to generate asymmetries in cell morphology and composition. To accomplish long-range transport, cells cannot rely on diffusion alone as many large organelles and macromolecular complexes are essentially immobilized by the dense meshwork of the cytosol. One strategy used by cells to overcome diffusion is to harness the free energy liberated by ATP hydrolysis through molecular motors. Myosins are a family of actin based molecular motors that have evolved a variety of ways to contribute to cellular organization through numerous modifications to the manner they convert that free energy into mechanical work.

Keywords: Unconventional myosin; Molecular motor; Actin; Duty ratio

1. Introduction

Myosins are characterized by three domains, a N-terminal motor or "head" that binds actin and ATP, a neck domain consisting of one or more light chain binding IQ motifs, and a C-terminal tail. Based on sequence analysis of motor domains, ~20 distinct classes have been identified [1]. However, a recent study examining the large number of newly completed genomes identified many more potential classes (a total of ~40) [2]. Unfortunately, the authors did not incorporate existing myosin phylogeny into their analysis making a direct comparison of the new myosins with previously identified classes difficult. A multitude of studies have indicated that the tail domains are critical for the functions of a given type of myosin [3]. However, the mechanochemical properties of motor domains have evolved unique characteristics and regulatory mechanisms to optimize function. Phylogenetic analyses have established that motor and tail domains may have coevolved, further suggesting that these domains are interdependent: i.e. the mechanical properties of a given motor domain are "matched" to the mechanical requirements of given function that is primarily dictated by the tail domain [4]. This review will focus on the wide diversity of mechano-chemical properties exhibited among members of the myosin family of actin based molecular motors and when possible try to relate these properties to the known or possible cellular functions of a given myosin. Although beyond the scope of this overview, it is important to note that the diversity of motor properties described here is further modulated by a wide range of regulatory mechanisms that can have profound impacts on the motor properties of a given myosin.

Over the past two decades, a number of assays have been developed to complement traditional biochemical studies of molecular motors. Among the most significant are the in vitro motility assays where motor-driven movement is reconstituted with purified proteins. This approach is designed to probe the mechanical properties of small groups of motors, or even single motor molecules. Combined with conventional biochemical approaches (transient and steady-state kinetics), these studies have provided detailed insight into how a motor converts the free energy liberated from ATP hydrolysis into mechanical work.

* Corresponding author. MCD-Biology, KBT 352, Yale University, PO Box 208103, New Haven, CT 06520-8103, USA. Tel.: +1 203 432 3469; fax: +1 203 432 6161.
E-mail address: mark.mooseker@yale.edu (M.S. Mooseker).

0167-4889/$ - see front matter © 2006 Elsevier B.V. All rights reserved.
doi:10.1016/j.bbamcr.2006.06.012

Table 1
Mechanochemical properties of selected myosins

Class		Duty ratio [a]	Landing rate	Rate limiting step	Velocity [b] (μm/s)	Directionality
I	Myo1a	0.05 [15]		Pi release [14]	0.05 [137], 0.1 [138]	Plus [156]
	Myo1e			Pi release [16]		
	Myo1b				0.137 [157]	
II	Skeletal muscle	0.038 [8], 0.05 [5]		Pi release	6.6 [8], 6.9 [5]	Plus
	Smooth muscle	0.04 [8]		Pi release	0.58 [8], 0.546 [158]	Plus
	Non-muscle myosin IIA	0.05 [c] [10]		Pi release [10]	0.3 [159]	Plus
	Non-muscle Myosin IIB	0.82 [c] [12], 0.4 [c] [11]		ADP release [12], Pi release [11]	0.092 [160]	Plus
III	Myo3				0.11 [161]	Plus [161]
V	Myo5a	0.7 [c] [43]	1 [105], 1.4 [162]	ADP release [43]	0.311 [105]	Plus [44,141]
	Myo5b	0.79 [c] [163]	1 [163]	ADP release [163]	0.22 [163]	Plus [163]
	S.c. Myo2p	0.2 [6]	5 [6]		4.5 [6]	
	D.m. MyoV	0.1 [c] [35]		Pi release [35]	0.46 [35]	
VI	Myo6 (monomer)	0.8 [c] [70]		ADP release [70,143]	0.058 [142], 0.131 [143]	Minus [142]
	Myo6 (dimer)			ADP release [143]	0.4 [71], 0.307 [143]	
VII	Myo7a	0.9 [c] [76]		ADP release [76]	0.16 [78], 0.19 [164]	Plus [78]
	Myo7b	0.8 [80,81]		ADP release [80,81]		
IX	Myo9b	1 [7]	1 [7,91]	ATP hydrolysis [92,93]	0.015 [90], 0.038 [7], 0.08 [91], 1.1 [111]	Minus [91], Plus [151]
X	Myo10	0.16 [30], 0.6, [165]			0.3 [104]	Plus [104]
XI	Myosin XI		1 [86]		4.6 [86]	Plus [86]
XIV	TgMyoA			ATP hydrolysis or Pi release, [150]	5.2 [150]	Plus [150]

[a] Determined from Eq. (1) or solution kinetics.
[b] Kron and Spudich assay [139] at maximum motor density.
[c] Duty ratio of single-headed construct.

In vitro motility assays provide us with a number of mechanochemical parameters that define the motor activity of each myosin, i.e. a mechanical "signature" that is unique to a given myosin. These include (but are not limited to), duty ratio, processivity, power stroke/stepping, velocity, and directionality. Table 1 summarizes many of the known values for these parameters among the myosins characterized thus far. This review is a survey of our current state of knowledge regarding these properties in myosins examined to date. The experimental strategies used to assess mechanochemistry will be discussed, with a focus on in vitro motility assays.

2. Duty ratio and processivity

2.1. Measuring the duty ratio

For a myosin, duty ratio is defined as the proportion of the ATPase cycle that the motor domain remains strongly bound to actin. It can be determined based on the proportion of myosin bound to actin at steady state, or calculated from rate and equilibrium constants of individual steps, if known, where myosin bound to ATP or ADP·Pi is a weakly bound conformation and ADP or nucleotide free states bind actin strongly (Fig. 1).

The empirical method for determining duty ratio using in vitro motility is by plotting filament gliding velocity as a function of motor density. As the number of low duty ratio motors is reduced, velocity slows due to the decreased probability that a motor is engaging in a productive interaction with actin (Fig. 2A, dotted and dashed curves). A high duty ratio motor, in contrast, will spend most/all of its ATPase cycle bound, and filament gliding velocity will not decrease over a wide range of densities (Fig. 2A, solid line). The functional relationship between velocity and motor density can be used to determine the duty ratio by the equation originally derived by Uyeda and coworkers [5] and modified according to Reck-Peterson et al. [6].

$$V(\rho) = V_{\max}[1 - (1-f)^{\rho \cdot \bar{A}}] \quad (1)$$

V is the average filament velocity as a function of density (ρ), $V_{\max}$ is the maximum gliding velocity, f is the duty ratio, and $\bar{A}$ is the area of interaction (defined as the product of twice the filament reach and mean filament length). For example, when Eq. (1) is used to fit a curve to velocity vs. density data for the *S. cerevisiae* class V myosin Myo2p[1] f is measured to be 0.2 [6]. In contrast, $f=1$ when velocity data for human Myo9b is fit with the same equation [7]. Thus, Myo2p is predicted to be attached to actin for 20% of each catalytic cycle, while Myo9b is attached throughout.

2.2. Low duty ratio myosins

Duty ratio varies widely among myosins (see Table 1) and has profound implications for cellular function. For skeletal and smooth muscle myosins II (Myo2) the value is between 0.04 and 0.05 [5,8] based on Eq. (1). Clearly, this is optimal for a muscle tissue, where large ensembles of heads bind to the same actin filament to produce rapid contraction. Heads must quickly

[1] In this review myosin classes are referred to with roman numerals, while specific myosins within a class are designated with Arabic numbers.

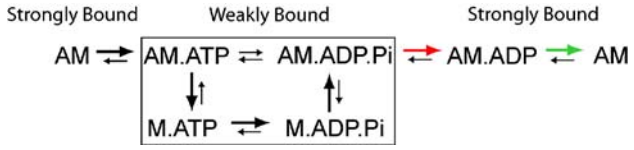

Fig. 1. Myosin ATPase cycle. Myosin (M) interactions with actin (A) are generalized as weak or strong, depending on the bound nucleotide. Slowing biochemical transitions can extend the duration of the "on" or "off" states. The two most common kinetic adaptations are limiting the rate of Pi (red arrow) or ADP (green arrow) release from the active site. Slowing these steps keeps the motor weakly bound or strongly bound, respectively, for a longer duration of its total cycle.

interact with the filament and detach so as not to interfere with the displacement activity of other heads. Muscle myosin achieves this low duty ratio by biasing the kinetics to the unbound/weakly bound state (myosin with ATP and ADP·Pi in the active site). It has high affinity for ATP and the rate-limiting step of the actin activated ATPase cycle is Pi release (Fig. 1, red arrow). As a result, heads spending the bulk of their cycle in the weakly bound state [9].

The situation appears to be slightly more complicated for vertebrate non-muscle Myo2 isoforms. A subfragment 1 (S1) Myo2a construct expressed in the baculovirus system (BV-expressed) has a low duty ratio similar to muscle myosin [10], while BV-expressed S1 Myo2b has a significantly higher duty ratio, depending on nucleotide and actin concentrations, with maximal values determined at 0.4 [11] to 0.82 [12]. This higher proportion of ATPase cycle time spent bound to actin is attributable to an increased affinity of ADP and a rate of ADP release approaching the steady-state ATPase [12]. The longer-lived attachment time of Myo2b is not suited for rapid contraction and may instead be an adaptation for generating tension. Support for this model was obtained through measurements of retrograde actin flow in neuronal growth cones from Myo2b knock-out mice. In the absence of Myo2b the rearward flow of actin in the lamellapodia occurs twice as fast relative to wild type cells [13]. Removal of Myo2b activity, which normally acts as a brake on retrograde flow, allows more rapid flow attributable to Myo2a.

Kinetic measurements of class 1 myosins including *Acanthomeba* myosin IA and IB [14], Myo1a [15], and Myo1e [16] indicate they are low duty ratio motors by a mechanism of rate limiting Pi release [14,16] . This class of myosins is involved in membrane binding, generation of cortical tension, endocytosis and organelle trafficking [3,17–21] as well as anchoring membrane proteins in lipid rafts [22]. To ensure that some Myo1 heads are interacting with actin these motors normally localize to regions of the cell that are rich with actin filaments such as the microvillus or lamellapodia/ruffles [21,23]. Myo1a (brush border myosin I) forms cross-links between the underlying actin core and the plasma membrane of intestinal microvilli [24]. Despite spending the majority of its ATPase cycle weakly bound to actin, Myo1a has much slower rates of ATP induced dissociation from actin and ADP release, compared to muscle myosins [15], although these steps do not limit the overall cycling rate. The extended lifetime of the actin-bound state is thought to contribute to its structural role in the microvillus. In the absence of Myo1a, knockout mice microvilli exhibit membrane and organizational defects consistent with this proposed function [25].

2.3. Moderate duty ratio myosins

Several myosins, such as those belonging to class X, fall into a category best described as moderate duty ratio. Class X myosins were first identified as a motor involved in tipward trafficking in filopodia [26]. More recent work has identified beta-integrins [27] and the actin nucleators Mena/VASP [28] as cargo delivered to filopodial tips by Myo10. An additional role for Myo10 in pseudopod extension during phagocytosis has also been proposed [29]. Kinetic analysis of a BV-expressed construct encoding the motor and light chain binding domains indicates it has a duty ratio of ~0.16 [30], requiring >6 motors to effectively move cargo. EM of negatively stained full-length

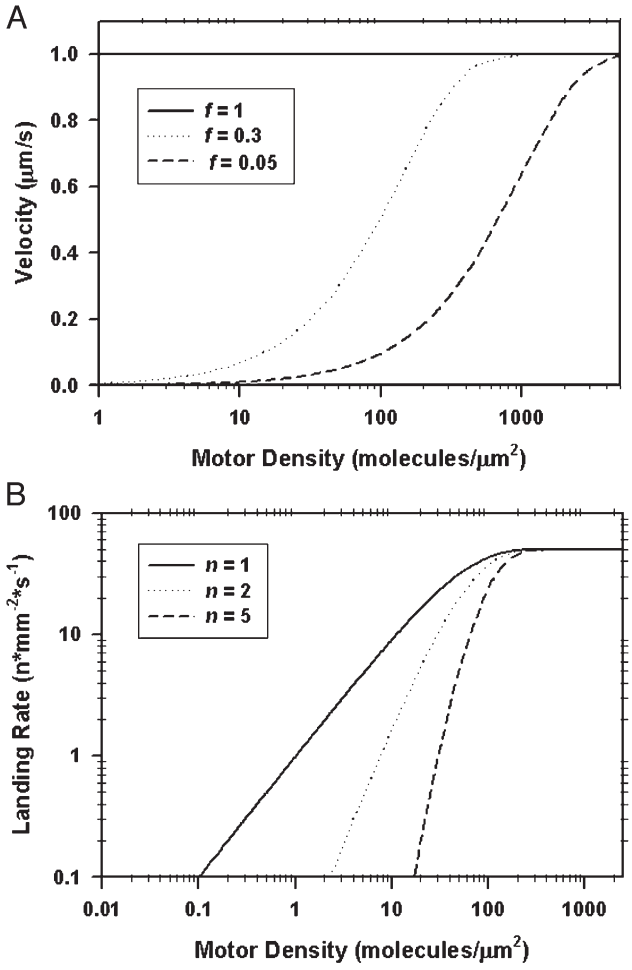

Fig. 2. Theoretical velocity and landing rate curves vs. motor density. (A) Using Eq. (1), theoretical curves of velocity vs. motor density were generated on a semi-log scale for high (f=1, solid line), moderate (f=0.3, dotted line) and low (f=0.05, dashed line) duty ratio motors with a maximal velocity of 1 μm/s. (B) Log–log plot of theoretical landing rate curves from Eq. (2) [99]. The minimum number of motors needed for a filament to successfully land and move is represented by n. Curves representing motors with n=1 (solid line), n=2 (dotted line), and n=5 (dashed line) are shown.

Myo10 suggests it is likely to exist predominantly as a monomer [31] and is unlikely to increase its duty ratio through dimerization of two moderate duty ratio heads.

Many class V myosins also have moderate duty ratios. *Drosophila* has a single gene for Myo5, also called *didum* [32,33], which functions during larval development and sperm individualization [34]. A single-headed *Drosophila* Myo5 BV-expressed construct was calculated to have a duty ratio of 0.1 by kinetic analysis and, accordingly, an expressed dimer exhibited properties of a low duty ratio in the in vitro motility assay [35]. While not directly measured, Pi release was predicted to be the rate-limiting step, which would keep Myo5 in a weakly bound state. In *Saccharomyces cerevisiae*, there are two class V myosins, Myo2p and Myo4p. Myo2p is involved in polarized secretion [36], inheritance of mitochondria [37] and vacuoles [38], and mitotic spindle orientation [39]. Myo4p transports mRNA to daughter cells during division [40] and is involved in cortical ER inheritance of daughter cells [41]. Quantitative analysis of velocity vs. density assays assigned a duty ratio of 0.2 to native, immuno-adsorbed Myo2p. Because motor density for Myo4p could not be determined, the duty ratio could not be calculated. However, it did exhibit slower velocities at lower concentrations of antibody used to tether it to the motility chamber, which is inconsistent with a high duty ratio [6]. There is no kinetic data for the yeast class V myosins to corroborate these results as of yet, but the motility data suggests multiple motors are required for the proposed long-range transport functions.

2.4. High duty ratio myosins

In contrast to yeast and *Drosophila* class V myosins, vertebrate Myo5a is a high duty ratio motor. Myo5a, perhaps the best characterized unconventional myosin, has a myriad of cellular functions ranging from retention/targeting of sooth ER in dendritic spines of Purkinje neurons to melanosome transport (reviewed in [3,42]). A duty ratio of 0.7 was calculated based on pre-steady state kinetics of a single headed expressed Myo5a construct [43]. The coiled-coil sequence in the tail of the native molecule results in dimerization of two high duty ratio heads into a functional unit [44], increasing the probability at least one head is attached at all times, consistent with reports that it rarely detaches from actin [45,46]. As a striking example of its high duty ratio, Myo5a velocities actually increase at low motor densities [47,48]. Multiple high duty ratio heads bound to the same filament likely interfere with each other and this interference is alleviated at low densities.

The high affinity of Myo5a for actin is achieved through a combination of structural and kinetic adaptations of the ATPase cycle. The rate limiting step is ADP release, ensuring that it populates the strongly bound state most of the time [43] (Fig. 1, red arrow). Furthermore, single molecule studies using optical trapping suggests detachment of the trailing head is coordinated with the leading head through intramolecular strain, [49,50] (see discussion of Myo5a stepping below). Such coordination also contributes to a high duty ratio by further increasing the probability that one head remains attached.

Myo5a has modifications to a small surface loop involved in actin binding as an additional mechanism to increase duty ratio. This region, referred to as loop 2, is positioned optimally to interact with actin [51]. A number of studies examined the role of loop 2 by altering the sequence and examining the resulting actin and nucleotide binding properties [52–54] . This work determined that the sequence of loop 2 regulates the affinity of Myo2 for actin. In particular, the addition of basic residues significantly increases the affinity of myosin for actin [52,54]. The Myo5a loop 2 is longer relative to Myo2, with a number of additional charged residues. The presence of additional lysine residues increases Myo5a affinity for actin in the M ADP·Pi state [55]. Similar results were obtained for *Drosophila* Myo5, as a splice variant with a shorter loop 2 displayed reduced affinity for actin [35]. A recent cryo-EM study examining the structure of Myo5a in various nucleotide-bound states attached to actin provided a mechanism for these observations. When weakly bound to actin (ATP and ADP·Pi states), loop 2 rearranges to make an electrostatic interaction with actin [56], acting as a tether.

Work from a number of groups suggests class VI myosins may also have a high duty ratio. Expression of this class of myosins appears to be restricted to metazoan animal species including *Drosophila*, where it was first discovered [57], *C. elegans,* and vertebrates [1]. Like class V myosins, class VI myosins are involved in a wide range of cellular functions including; cell migration [58,59], clathrin-mediated endocytosis [60–62], and Golgi maintenance [63,64]. In addition, deafness [65–68] and cardiomyopathy [69] are two diseases linked to mutations in Myo6.

Initial solution kinetic experiments on a single-headed (S1), BV-expressed Myo6 construct assigned a duty ratio of 0.8 [70]. Myo6 has adaptations similar to Myo5a, with high affinity for ADP and rate-limiting ADP release [70,71]. Due to the presumed coiled-coil sequence in the tail, it was predicted that the heads would dimerize in a manner similar to Myo5a, and this combination of two high duty ratio heads would produce a motor with a duty ratio ~1, a property associated with motors involved in long distance transport. This was supported by results from processivity assays with this motor (see below). However, the BV-expressed constructs used in these studies included exogenous, engineered domains that forced heavy chain dimerization. Subsequent work using cross-linking and hydrodynamic measurements demonstrated that native Myo6 is, in fact, a monomer [72]. Filament gliding velocity of a BV-expressed full-length construct decreased as the density was reduced in the in vitro motility assay, indicating it has a duty ratio of less than 1 [72]. Class VII myosins are the most recently identified as possessing a high duty ratio. Mutations in Myo7a are associated with several forms of inherited deafness and deaf-blindness in both humans and mice [73,74]. Additionally, a new role for Myo7a has also recently been suggested in trafficking of lysosomes [75]. A recent study found a single-headed construct encoding *Drosophila* Myo7a has the unusual property of hydrolyzing ATP when bound to actin [76], coupled with ADP as a rate limiting step. Based on kinetic measurements, a duty ratio of 0.9 was assigned to the single-headed molecule.

Analysis of the primary structure of Myo7a indicates the likely formation of a coiled-coil into a highly processive dimer [77]. Consistent with this prediction is a report that full-length, BV-expressed rat Myo7a runs as a dimer during native gel electrophoresis and gel filtration chromatography [78]. Interestingly, an expressed construct encoding the head, neck and coiled-coil region, but lacked the more C-terminal portion of the tail, did not dimerize. This implicates regions other than coiled-coil in promoting dimerization of Myo7a, but it has not been determined if they are sufficient [78]. The other class VII isoform, Myo7b, localizes to the brush border microvilli of enterocytes lining the gut and proximal tubule epithelial cells [79], but its cellular functions are largely unknown. Single-headed (head and neck) BV-expressed constructs of both mouse and *Drosophila* Myo7b have a duty ratio of 0.8 and rate limiting ADP release based on the pre-steady state kinetics [80,81]. While there is no predicted coiled-coil in the sequence of this myosin, it cannot be assumed Myo7b is monomeric given the requirement of other sequences for dimerization of Myo7a as noted above. Plants have three classes of myosins, VIII, XI, and XIII, all of which are probably evolutionarily related to class V myosins [2]. Only the mechanochemistry of class XI myosins, has been investigated. Little is known regarding its function beyond its involvement in the cytoplasmic streaming of organelles. Myosin XI expressed in the filamentous algae *Chara* is the fastest myosin described to date, moving filaments at 100 μm per second in vivo and 60 μm per second in vitro [82]. Myosin XI has been implicated in transport of mitochondria, plastids, and peroxisomes based on co-localization [83,84]. Overall, its organization is very similar to Myo5a, with a long light chain binding domain and coiled coil region [85]. Filament gliding velocity does not decrease over a wide range of Myosin XI densities, and ADP inhibition of motility suggests a high ADP affinity, both characteristic of a high duty ratio myosin [86] and supportive of the model whereby Myosin XI is ideally suited for long range transport of vesicular cargo.

The final class of myosins for which the duty ratio has been measured is class IX. Class IX myosins are unique due to a functional GTPase activation protein (GAP) domain within the tail domain [87–90]. The cellular function(s) for class IX myosins is not known, although it is presumed to participate in Rho-dependent remodeling of the actin cytoskeleton. Consistent with this idea is the observation that vertebrate Myo9b is most highly expressed in motile cells such as leukocytes [89]. The tail domain of class IX myosins does not contain a coiled-coil sequence. Hydrodynamic analysis and chemical cross-linking confirmed it functions as single heavy chain with associated light chains [7]. Initial studies on Myo9b demonstrated that this myosin, like Myo5a [45,46], binds to F-actin in both the absence and presence of ATP, a property indicative of a high duty ratio [90]. This was later confirmed for both the native Myo9b and a truncated (lacking most of the tail including the GAP domain) BV construct where a fit of velocity vs. density measurements gave a duty ratio of ~1 [7,91] .

Interestingly, the kinetic properties of Myo9b are quite different from those of other high duty ratio myosins. Myo9b has a low affinity for ADP and rate limiting ATP hydrolysis [92,93]. Therefore, other modifications to the motor domain are likely to account for its high duty ratio. Specifically, there is a 126 amino acid insert in sequence corresponding to loop 2 that is rich in basic residues with a calculated isoelectric point of 11.6 [89]. This region may function as an electrostatic tether [7], similar to that reported for the processive, single headed movement of the kinesin KIF1A along microtubules [94]. Accordingly, deletion of the insert lowers Myo9b's affinity for actin. [92]. In addition to loop 2 modifications, Myo9b has an N-terminal extension of 60 amino acids relative to myosin II. Deletion of this extension also reduced actin affinity [92]. Based on the crystal structure of the motor domain of skeletal muscle myosin II [51], this insertion is predicted to be near the head–neck junction, an unlikely position to influence actin binding through a direct interaction. Instead, this domain could affect nucleotide binding, product dissociation, or lever arm movement/rotation.

2.5. Determining processivity

Processivity is a mechanochemical property closely associated with duty ratio and refers to the number of catalytic cycles a motor can perform before diffusing away from its track. For highly processive motors, hundreds of rounds of ATP binding and hydrolysis can occur before release from actin while non-processive motors will bind actin once per ATPase cycle and release. The most straightforward assay for characterizing processivity is through the direct observation of single molecule motility [95]. However, this approach requires sensitive microscopy instrumentation and the ability to precisely label motor molecules with known stoichiometry. In one such assay, the movement of single myosins labeled with GFP or fluorescent light chains along surface-bound actin is recorded by total internal reflection (TIRF) microscopy [95–98]. Continuous single-molecule translocation is an indicator of processive behavior. For example, single dimeric Myo6 motors can move longer than 200 nm without detaching [97] and Myo5a "runs" can extend several microns [96].

The landing rate assay is routinely used to determine the minimum number of myosins required to capture and move a filament, which for a processive motor will be 1 [99]. In this assay, the number of filaments that land and move in a field per second is determined over a range of densities. Eq. (2) is used to fit a curve describing the behavior of landing rate with respect to motor density to the log–log plot of the data. Solving Eq. (2) for n gives the minimum number of motors required for motility (Fig. 2B).

$$L(\rho) = Z(1 - \exp^{-\rho \cdot \bar{A}})^n \quad (2)$$

L is the landing rate as a function of motor density (ρ), Z is the maximum landing rate, $\bar{A}$ is the area of interaction (defined as above), and n is the number of motors required for a filament to land and move. A best-fit curve, with Z, $\bar{A}$, and n as free parameters, will provide the landing rate. However, n is commonly set to 1 or 2, and the error associated with the fit of each curve to the data used to assign the landing rate. The

reciprocal of this number is frequently taken as the duty ratio. For example, for a motor with a landing rate of 2, the duty ratio is presumed to be less than 1, but greater than or equal to 0.5. However, the relationship between landing rate and processivity does not always correlate, that is, $1/n$ may not be equivalent to f (from Eq. (1)). The axonemal inner-arm dynein c of *Chlamydomonas* has a low duty ratio of 0.14 calculated based on velocity vs. motor density measurements yet a fit of the landing rate data indicates one molecule is sufficient to move a microtubule [100]. The mechanism of this seemingly contradictory behavior is still unknown. Clearly there are motors whose activity cannot be described within the parameters defined by conventional assays.

Processive movement by a single myosin can be confirmed with the observation of nodal point pivoting, which occurs when an actin filament is tethered by a single motor while the ends are free to diffuse [47]. Averaging the fluorescence intensity from successive intervals will reveal a single bright spot, corresponding to the site of motor attachment. This behavior is not observed for non-processive motors where velocity decreases at lower densities and attachment of moving filaments at a single point cannot occur.

Optical trap studies of single motors can provide a more detailed look at the mechanism of processivity. The three-bead assay, in which a filament trapped between two beads is brought into proximity of a platform bead coated with single motors, provides the most detailed information [48,101]. Processive motors, upon binding to the suspended filament, will displace the trapped bead(s) repeatedly without detaching, resulting in "staircase" plots of displacement vs. time [47,97,98]. Non-processive motors will bind and undergo a single displacement event. Moreover, the nucleotide-dependence of acto-myosin interactions in this assay also provides valuable information regarding the biochemical transitions of the motor.

2.6. Non-processive myosins

In general, there is a strong correlation between duty ratio and processivity. Class II myosins are non-processive, exhibiting reduced gliding velocities at low motor density [5,8] and single displacement events with optical trap measurements [102]. Two class I myosins, Myo1a and Myo1b, are also non-processive in single molecule assays [103]. Moderate duty ratio myosins such as Myo10 and invertebrate class V myosins exhibit decreased gliding velocities at low motor densities [6,35,104]. However, velocities fall off at lower densities than for muscle Myo2, consistent with a moderate duty ratio myosin that is non-processive.

2.7. Processive myosins

Based on landing rate, run lengths of single molecules with TIRF microscopy, and optical trapping experiments a number of myosins exhibit highly processive movement, a property ideal for a motor involved in long range transport. Myo5a, initially isolated from chick brain [44], was the first myosin discovered to exhibit highly processive movement. Filament landing rates as a function of Myo5a density, coupled with nodal point pivoting and multiple displacements in the optical trap assay, demonstrated single molecules of Myo5a were capable of sustaining filament movement [47]. In support of these data, single Myo5a molecules labeled with fluorescent calmodulin light chains can moves on surface-bound actin filaments for many microns [96]. Differences in the loop 2 sequence of class V myosins appear to explain the reported discrepancy in processivity between vertebrate and invertebrate isoforms [6,35,105]. Loop 2 in the mouse Myo5a sequence has a net charge of +6, while the same region in the yeast class V myosin Myo4p is shorter with no net charge. When the loop 2 sequence from Myo4p was incorporated into mouse Myo5a-YFP the chimera appeared processive at low ionic strength, with TIRF run lengths and a landing rate consistent with processivity. However, as ionic strength approached physiological levels, chimeric motor run lengths decreased and $n=40.3$ motors were determined to be required for filament movement based on the landing rate assay. Wild type Myo5a was processive under all conditions [106], underscoring the importance of electrostatic interactions/tethering between loop 2 and the actin filament in increasing Myo5a's duty ratio and processivity [55,56,106].

One current controversy in the myosin field is whether or not Myo6 functions as a processive dimer. The characterization of this myosin's motility initially relied on constructs including sequences forcing it to dimerize [97,98]. These engineered, two-headed Myo6's were processive based on single molecule trapping studies and imaging of single molecule runs along actin with TIRF [97,98]. The discovery that Myo6 is monomeric suggested it may not by highly processive [72] given the duty ratio of a single head is less than 1 [70]. Accordingly, a BV-expressed wild type Myo6 encoding the entire motor exhibits single interactions/displacement events in the three-bead optical trap assay [72]. Interestingly, when the geometry of the optical trap setup is altered, processive movement of single-headed BV-expressed Myo6 was reported to occur [107]. In this experiment the trap is used to position a bead with a single motor on a stationary actin filament (instead of positioning the filament on a stationary motor) and the bead displacement monitored. The resulting multiple stepping events of single-headed Myo6 in this configuration are proposed to result from diffusional restriction imparted by the large bead. That is, the bead "holds" the Myo6 motor near the actin filament until it re-attaches. It now appears that, under certain conditions, in vitro BV-expressed Myo6 encoding the full-length wild type sequence can form dimers. When these motors were clustered on actin filaments 17% of Myo6 molecules were two-headed as evidenced by rotary shadowing EM. Furthermore, 15–30% of BV-expressed wild type Myo6 with flourescently labeled calmodulin light chains moves processively along surface-bound actin by TIRF microscopy. Removal of the C-terminal cargo-binding domain increases the probability of Myo6 dimerization up to 90%, suggesting this region of the molecule may function to regulate the oligomeric state [108]. In vivo, several other mechanisms could bring Myo6 motors in close proximity to facilitate dimerization (Fig. 3). For example, a number of proteins interact with the tail domain of Myo6

(reviewed in [109,110]). Binding of two Myo6 heavy chains to one of these could induce a functional dimer (Fig. 3B). Alternatively, interactions with vesicular cargo could cluster enough Myo6 molecules to result in coiled-coil formation into a true dimer (Fig. 3C) or a functional dimer of two motors in close proximity (Fig. 3D).

The final class of processive myosins described so far is class IX myosins, which are single-headed [7,91]. Processivity is commonly associated with two headed motors that coordinate their activity so that one head remains attached to actin while the other is unbound. Thus, it was somewhat of a surprise that the Myo9b landing rate was measured as $n=1$ and nodal point pivoting was observed [7,91]. A BV-expressed Myo9b motor without a tail domain takes multiple steps in the optical trap assay and single Myo9b-GFP fusion proteins moved along actin filaments for hundereds of nanometers when visualized by TIRF [111]. It will be of interest to determine if a processive, single-headed motor can move when an opposing load is applied in the optical trapping assay. As discussed above, the inserts in the motor domain of this myosin are likely to play a role in tethering the molecule to prevent diffusion during its weakly bound states, compensating for the lack of a second head and facilitating processive movement [92].

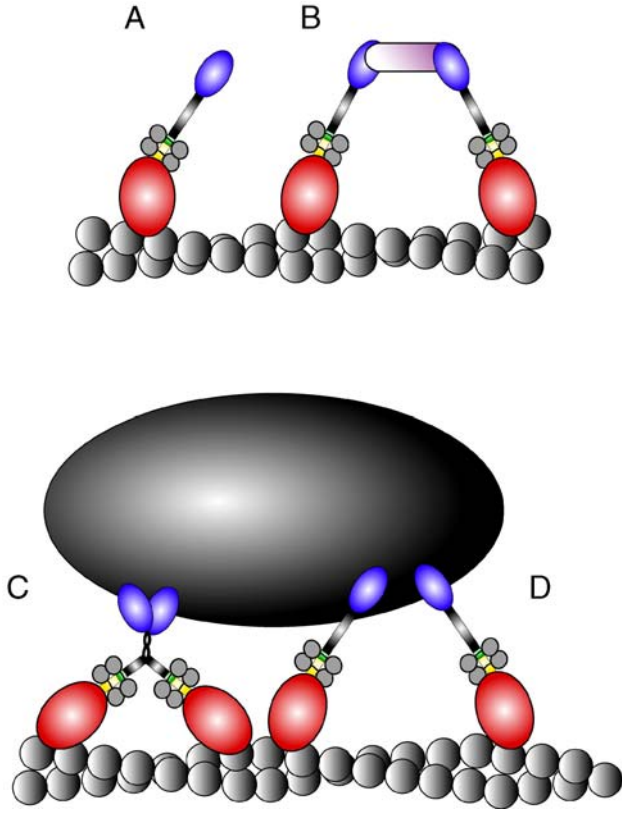

Fig. 3. Possible states and mechanisms of Myo6 oligomerization in vivo. (A) Myo6 might function exclusively as a monomer or (B) binding of two Myo6 motors to the same (or complexed) tail interacting protein(s) could induce the formation of a functional dimer. (C) Vesicular cargo could act as a recruitment platform for Myo6 with dimerization occurring once enough motors are concentrated (C), or two monomers in close proximity could work together as a functional dimer (D).

3. Power stroke/stepping

X-ray diffraction studies of muscle led to the proposal of the swinging crossbridge model of contraction in which the movement of actin occurred through the rotation of some structural components of the actin-bound myosin followed by release of the filament [112]. The kinetic mechanism of Lymn and Taylor provided a biochemical explanation of how the cycle worked by assigning a nucleotide state to each conformation of myosin. The first crystal structure of myosin II identified the potential rotational element as the light chain binding, alpha-helical neck domain emerging from the motor domain [51]. Crystallographic studies of muscle myosin II in various nucleotide-bound conformations [113–117] support the hypothesis that this region undergoes a rotational movement, thereby acting as a lever arm that exerts a power stroke, during the weak to strong ($ADP{\cdot}Pi \rightarrow ADP$) binding transition. For a detailed review of the lever arm mechanism of myosin II, see [101].

Single molecule studies of two unconventional myosins, Myo5a and Myo6, have provided detailed insight into the mechanism whereby two-headed motors have adapted their power stroke during processive movement. Optical trapping studies provided the basis for the stepping model of processive, two-headed myosin motility when it was observed that single Myo5a dimers displaced the trapped beads in 36 nm increments [105], corresponding to the binding site repeat along the actin filament. Negatively stained EM of Myo5a also showed conformations with both heads attached and spanning 36 nm [118]. Furthermore, the size of the displacement of Myo5a stepping in single molecule assays depended linearly on the length of the light chain binding domain [119,120]. This relationship between increased displacement and light chain binding domain length is in remarkable agreement with the lever arm model. Furthermore, these studies were taken as strong evidence by most that Myo5a took sequential steps along actin, in a hand over hand fashion.

Alternative models were proposed to account for the 36 nm displacements of Myo5a. The inchworm model, put forth to explain the movement of kinesin [121], argues that the relative position of the heads (i.e. leading vs. trailing) does not change. The Brownian ratchet model postulates that motors slide along the filament to low energy binding sites [122]. Advances in detecting fluorescence of single fluorophores with high spatial and temporal resolution allowed the hand over hand model to be tested directly. By measuring the rotation of a CaM light chain labeled with a fluorophore in a known orientation, Forkey and colleagues detected tilting of the light chain binding domain as predicted for a lever arm swinging between pre- and post-power stroke states [123]. The development of a technique referred to as FIONA (Fluorescence Imaging with One Nanometer Accuracy), which can follow single fluorophores with <1.5 nm resolution, also provided strong evidence for the hand over hand mechanism. In this study, the position of a single, fluorescently labeled light chain near the motor domain of one head was tracked during Myo5a movement on actin. The hand over hand model predicts that for each 36 nm center of mass displacement, the trailing head will detach, pass over the

leading head and re-bind actin 74 nm from its initial position. Indeed, Yildiz et al. observed alternating steps of 74.1±2.2 nm [124]. Similar results were obtained when the two heads of Myo5a were labeled with different colored quantum dots to track the position of the heads with high temporal and spatial resolution [125].

Hand over hand processive movement would be enhanced if the heads could "communicate" with each other to coordinate their ATPase cycles. To explain the extraordinary run lengths demonstrated by some unconventional myosins, stepping models incorporate mechanisms of coordination to increase the probability that at least one head will always remain bound to actin. Backward strain exerted on the leading head by the trailing head was proposed to be the mechanism by which coordination occurred [70,126]. Consistent with this model, the leading head of Myo5a was observed to curve backward when both heads were attached [118]. Two recent studies have explored the effect of strain on single Myo5a molecules in the optical trap assay to test this model. For these studies, single headed Myo5a constructs were subjected to pushing or pulling forces exerted on the actin filament-bead "dumbell" by the trap. These forces are presumed to correspond to the load imposed on the trailing and leading heads, respectively [49,50]. Both groups report that pulling backward on the motor slows ADP release from the leading head, keeping it locked in an early stage of actin binding and effectively preventing it from releasing actin. Veigel and coworkers also report a twofold reduction in the lifetime of actin binding when forward, or "pushing" force is applied. Extrapolating to a two-headed molecule, this result suggests the force applied to the trailing head by the leading head accelerates ADP release, ATP binding, and dissociation. These studies present convincing data that strain dependent kinetics keep the ATPase cycles out phase and contributes to processivity.

Expressed Myo6 engineered to form a two-headed dimer also moves processively in the optical trap assay, with a large (30–36 nm) step size [97,98]. A hand over hand model of stepping, similar to that for Myo5a, was proposed to account for its movement. The FIONA technique of imaging the displacement of single fluorescently labeled heads confirmed this mechanism. Motor domains were displaced 60 nm [127] or 72 nm [128] for each 30–36 nm movement of the center of mass, exactly as predicted by the hand over hand model.

The mechanism of two-headed Myo6 stepping has been considerably more complicated to elucidate since the initial observation was made that the 30–36 nm step size of Myo6 is considerably larger [97,98,129] than would be predicted based on a short lever arm occupied by only one CaM light chain (which follows the unique 53 amino acid-nonIQ CaM binding insert thought to be critical for minus end directionality of Myo6 [129]. Moreover, inter-head binding distances of GFP-labeled motor domains demonstrated separation of ~30 nm under near rigor conditions [130]. Within the constraints of the hand-over-hand stepping model, two possibilities were proposed to account for the large displacement of Myo6. The first postulated an extension of the lever arm through some a rigid element, such as the 53 amino acid insert proximal to the light chain-binding domain. The second relied on the existence of a flexible element, allowing the dimer to unfold and search out the next binding site. This second mechanism was supported by the "promiscuous" nature of Myo6 binding to actin at slightly irregular intervals [97]. Closer inspection of the predicted coiled-coil immediately C-terminal to the IQ motif revealed only a modest propensity to dimerize, suggesting this region could form the flexible element [127,131,132]. To test this directly, this region was "zipped up" by the addition of a GCN4-p1 dimerization sequence [133]. Addition of this sequence resulted in a dramatic decrease in dimeric Myo6 step size down to 12 nm, the same magnitude displacement as single-headed constructs [132].

The effects of load on Myo6 stepping have also been examined for a two-headed, BV-expressed construct with optical trapping. Under physiological ADP and ATP concentrations (100 μM and 1.5 mM, respectively), even very small loads accelerated the rate of ADP binding and stalled Myo6 on the actin filament [131]. Thus, two-headed Myo6 may function as a tether, anchoring vesicles or other cargo to the actin cytoskeleton.

An expressed, full-length Myo6 monomer exhibited single binding and displacement events of 18 nm [72], still longer than the calculated light chain binding domain length of 10 nm [132]. Thus, even the power stroke of single-headed Myo6 likely depends on other, undetermined, structural elements. Determining if and how the oligomerization state of Myo6 is regulated is of critical importance in defining the in vivo functions of this motor.

The mechanics of the power stroke of class I myosins has also been investigated [103]. In the optical trap assay, single-headed myosins rat liver Myo1b and chicken intestinal brush border Myo1a undergo single displacements along actin before detaching. Importantly, these encounters were significantly longer than for other low duty ratio myosins, consistent with the slow ATPase cycles of Myo1a and the slow rate of ADP release [15]. Both myosin I's displaced actin 10–11 nm, but did so in two distinct phases [103]. The first 6 nm movement occurred rapidly after actin binding, while the second, 5.5 nm phase occurred at variable intervals later. Interestingly, the first phase is insensitive to ATP suggesting the rate of ADP release governs its duration. The duration of the second phase is dependant on the concentration of ATP and represents the rate of ATP-induced dissociation of the myosin from actin. Thus, the single molecule studies on active motors support the structural data which suggest there is a second component of the Myo1a working stroke coupled to ADP release [134].

This bi-phasic mechanical working stroke is not limited to class I myosins. Another single headed myosin, an S1 fragment of smooth muscle myosin II, was reported to displace actin in two steps (4+2 nm). Application of backward load increased the duration of the first phase, thus increasing the overall attachment time, but had little effect on the second phase [135]. Bi-phasic stepping also contributes to the movement of the two-headed myosin, Myo5a. The first component of the step is due to 20 and 5 nm sub-steps of the leading head, with a 10–11 nm diffusive search by the unattached head for the next binding site [136]. It now seems likely that a two-step working occurs in those

myosins whose ADP release rate is strain-dependent. The second conformational change would be inhibited in the presence of backwards strain, preventing ADP release and lengthening the lifetime of the strongly bound state.

4. Velocity

The velocity at which a myosin moves along an actin filament is defined by three parameters, the displacement per ATP hydrolyzed (step size *d*), the duty ratio (*f*), and the overall cycling rate (actin activated ATPase).

$$V = \frac{d \cdot k_{\mathrm{ATPase}}}{f} \tag{3}$$

Independent measurements of these three parameters can be used to calculate a velocity that is frequently in good agreement with experimentally determined values, although there are exceptions. For example, based on Myo1a measurements of $d \sim 11$ nm [103], $k_{\mathrm{ATPase}} \sim 0.3\ \mathrm{s}^{-1}$, and $f = 0.05$ [15] a velocity 66 nm/s is calculated with Eq. (3). This corresponds well to the experimentally determined velocity of 50–100 nm/s [137,138]. An astonishing range of velocities has been reported for different classes of myosins using in vitro motility, covering several orders of magnitude (see Table 1). Myo9b is the slowest, moving at 15–40 nm/s [7,90] while a class XI myosin from *Chara* moves 60 μm/s [82]. The gliding filament assay of Kron and Spudich, where the movement of fluorescently labeled filaments moving on motors attached to a coverslip is recorded, is the simplest and most routinely used method to measure the unloaded velocity of a myosin [139]. It should be noted that alternative assays of myosin motility can give dramatically different results, most likely due to motor orientations that are more or less favorable for filament interaction [140,141]. A striking example of this are studies examining the velocity of Myo9b. Initial studies of Myo9b using the gliding filament assay revealed it to be a relatively slow motor with velocities of 15–40 nm/s [7,90,91]. However, recent studies visualizing the movement of GFP-tagged Myo9b on immobilized actin filaments revealing much faster velocities ranging from 0.5 to 2 μM/s [111].

For a number of myosins there is a very clear relationship between the velocity, duty ratio/processivity, and physiology. A classic example is the different velocities of myosin II isoforms in skeletal (fast) and smooth (slow) muscle myosins. Smooth muscle myosin velocity in vitro is >10× slower than skeletal muscle myosin consistent with the much slower rates of smooth muscle contraction (0.58 μm/s and 6.6 μm/s, respectively) [8], while the low duty ratio of both is critical to prevent the large number of heads from interfering with each other during force generation. To transport cytoplasmic cargo over long distances a fast, highly processive motor would be most effective. Class XI myosins in plants are an idealized example. Their extremely rapid, and highly processive motility allow for the rapid cytoplasmic streaming of vesicles [82,86].

Several myosins are proposed to act as cellular anchors, tethering components in place to provide substructure. For a myosin to provide such a function, it would be advantageous to reduce, or even eliminate, its movement along actin. Based on Eq. (3), this could be accomplished by reducing the cycling rate, decreasing the step size, or increasing the duty ratio. Myo7b is an ideal candidate to operate in such a fashion in the highly ordered microvilli of the intestine and kidney proximal tubule epithelium, where it is localized [79]. Myo7b exhibits an extremely slow rate of actin activated ATPase rate (~1/s), coupled with a high duty ratio (0.8) [80], which is predicted to allow this motor to anchor microvillar components.

Some myosins may adapt their rate of movement on actin to perform multiple functions. It is now well established that load applied by an optical trap against the direction of single myosin movement can reduce the rate of stepping and, therefore, velocity by slowing biochemical transitions [49,50,135]. Myo6, for example, is involved in trafficking of vesicles during clathrin-mediated endocytosis (reviewed in [109,110]). Under the unloaded conditions of the sliding filament assay, Myo6 actin translocation rates are moderately fast for both single-headed and dimeric constructs, ranging from 80 to 300 nm/s in the absence of Ca^{2+}[71,142,143]. Myo6 is involved in the maintenance of stereocilia, specialized microvilli with a core bundle of actin filaments. Mice with a mutation in the Myo6 gene are deaf, have destibular dysfunction and prior to hair cell degeneration exhibit fused stereocilia [144]. The localization of Myo6 to the base of the stereocilia suggested it tethers the apical membrane [145] to the underlying actin meshwork. For this function, Myo6 mechanochemistry must be altered to convert it from a cargo mover to an anchor. Initial studies using an optical trap indicated that when a backward load is applied, Myo6 stalls and then quickly detaches [97]. Under these conditions, Myo6 occasionally steps backwards, but backward steps are followed by forward steps or detachment. When a physiological concentration of ADP is included in the assay load inhibits detachment and promotes a strongly-bound stalled state (i.e. velocity is 0 nm/s), consistent with an anchoring function. Removal of the major plus-end motor of the microvilli, Myo1a, induces loss of Myo6 from the apical domain [25]. This raises the possibility that in vivo, load is applied to Myo6 by Myo1a through the core actin bundle or membrane, thereby converting Myo6 to a microvillus tether.

5. Directionality

Actin filaments have an inherent polarity with a fast growing plus (barbed) end and a slower growing minus (pointed) end. Additionally, filaments within the cytoplasm are organized in a polarized fashion, with plus ends typically oriented towards the plasma membrane and minus ends towards the interior. The direction of myosin movement on actin, therefore, has profound implications for function. For example, a myosin involved in trafficking vesicles to the plasma membrane during secretion would necessitate plus-end-directed movement.

Three assays have been used to assess directionality of myosins (Fig. 4). The assay developed first for Myo5a relied on uniformly polarized bundles of actin filaments from the alga *Nitella* as a substrate for motility [146,147]. Beads with surface

bound motors are applied to the exposed cytoplasm of algae that have been cut open. Movement of the beads along the uniformly polarized actin bundles is recorded by time-lapse microscopy. Beads coated with a control motor, usually a known plus-end-directed myosin, are then imaged moving on the same bundles, thereby establishing its polarity [44]. One potential problem with this assay, aside from the relative technical difficulty in making the *Nitella* preparation, is that velocities of bead movement are much slower than that observed using the gliding filament assay [140]. A similar assay was developed with acrosomal actin bundles isolated from *Limulus* sperm [148]. These bundles are comprised of parallel 50–80 μm actin filaments organized by the protein scruin [149]. The bundles themselves cannot support myosin motility due to the presence of scruin, but serve instead as a template. Nucleation of actin from the plus end of the bundles, and their subsequent labeling with phalloidin results in a "broom" structure visible by fluorescence and easily distinguishable from the tightly packed bundle. Beads coated with a myosin are positioned on the broom with a laser trap and their movement observed by differential interference microscopy (DIC) [141]. Movement away from the bundle, toward the splayed end of the broom indicates plus-end-directed movement. Conversely, if the bead moves toward the tapered end it is a minus-end-directed motor. Although the assay based on *Limulus* actin bundles is effective at determining directionality, it requires an optical trapping system to efficiently position motor-coated beads on the filaments. A simpler approach was devised using motors attached to a coverslip [139] and filaments tagged at one end with a fluorescent label [142]. Tags are created by restricting nucleation off of pre-existing fluorescently-labeled (e.g. using fluorochrome labeled actin subunits or fluorescent phallotoxin) actin seeds. This is accomplished by carrying out elongation at concentrations of actin below the critical concentration of minus end growth [142], or by using capping proteins that effectively block elongation from the plus end [150,151]. Fluorescent phalloidin (of a different color than that used to label the seed) is then added to label the nucleated end. Time-lapse imaging of the polarity tagged filaments by surface-bound motors reveals the directionality of the motor in question. A myosin whose direction of movement is known should be used to verify the accuracy of the polarity tag since annealing events in solution and subsequent breakage events during in vitro motility can affect the apparent location of the tag.

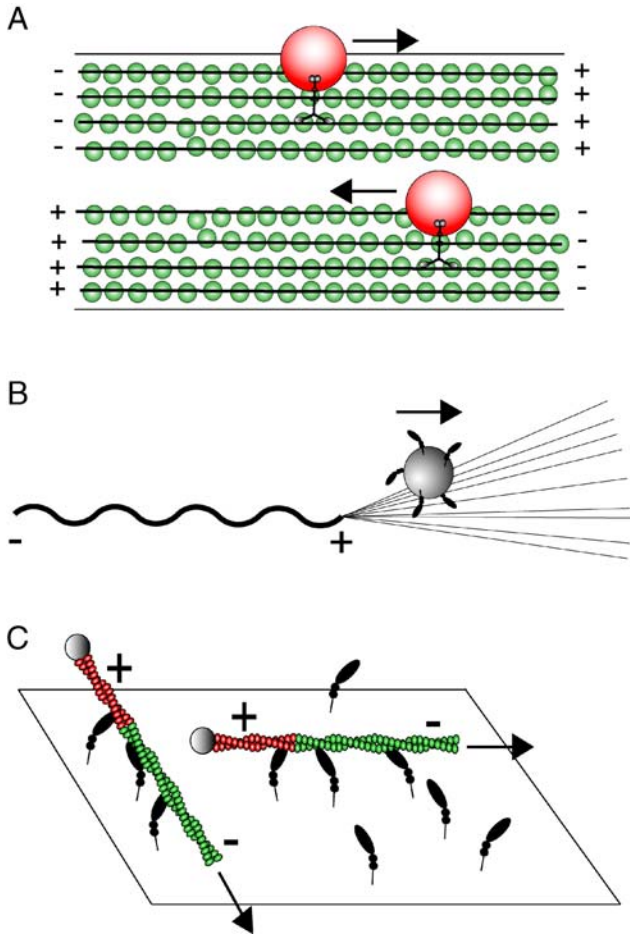

Fig. 4. Assays to determine myosin directionality. (A) Cells from the alga *Nitella* are cut open and pinned down with the polarized actin bundles in each half exposed to solution. The movement of myosin-coated beads along the cables is compared to a control motor to assess the polarity of the actin. (B) Nucleation from the plus ends of actin bundles from *Limulus* acrosomal processes creates a "broom" of known polarity. Myosin-coated beads are positioned on the broom with an optical trap. (C) In the gliding filament assay [139] actin filaments are fluorescently tagged on one end by polymerization off of the minus end of seeds whose plus ends are occluded by gelsolin (grey sphere). These are imaged moving on a coverslip coated with myosin and the trailing end indicates the directionality of the myosin.

Most of the myosins characterized to date are plus-end-directed (see Table 1). Single-headed Myo6 expressed in baculovirus was the first myosin described to move toward the minus end of actin [142], consistent with its proposed roles in trafficking vesicles toward the interior during clathrin-mediated endocytosis and anchoring the membrane between stereocilia of the inner ear [109]. Tail-less BV-expressed Myo9b is also reported to move to the minus-end of actin [91]. However, native Myo9b moves to the plus end [151] of actin and it is not clear why this discrepancy exists. The absence of the tail or method of attachment to the motility chamber (direct adsorption vs. immuno-adsorption) are possible explanations. To directly test whether removal of the tail converts Myo9b to a minus-end-directed motor, the directionality of a truncated CFP fusion immune-adsorbed (using a GFP antibody) from Cos cell supernatants was assessed. This fusion was plus-end-directed, similarly to the full-length native motor (Fig. 5). Thus, the simple presence vs. absence of the Myo9b tail cannot explain the observed differences in directionality of this motor. Given the large number of new myosin classes recently identified by genome analysis [2], it will be critical to determine if any others support minus-end (or bi-directional) movement.

The lever arm model of force generation predicts that, for a minus-end-directed motor such as Myo6, the lever arm will swing toward the minus end of actin. Initial cryo-EM reconstructions of actin filaments decorated with Myo6 in an ADP or nucleotide free state (representing the post-power stroke conformation) supported this model [142]. The authors also proposed the idea that the unique 53 amino acid insertion between the converter and lever arm regions is ideally

positioned to cause the re-orientation of the lever arm relative to other myosins. However, this model was challenged by experiments examining the directionality of chimeric BV-expressed constructs. Different combinations of motor, converter, and lever arm domains from Myo6 and Myo5a were expressed to probe the determinant of directionality using polarity tagged filaments in the in vitro motility assay [152]. This study concluded that the minimum requirement for minus-end-directed motility is the core of the Myo6 motor domain and did not depend on its unique converter or lever arm.

More recently, several papers provided strong evidence to support the original model of Wells et al. [142]; the reverse orientation of the lever arm is responsible for reversing Myo6 directionality. To directly test this hypothesis a normally plus-end-directed myosin, *Dictyostelium* class I MyoE, was engineered so that an artificial lever composed of α-actinin repeats was reversed 180° relative to the wild type lever arm by inserting a four helix bundle from human guanylate-binding protein-1 between the motor and lever arm [153]. This construct moved toward the minus end of polarity-tagged filaments,

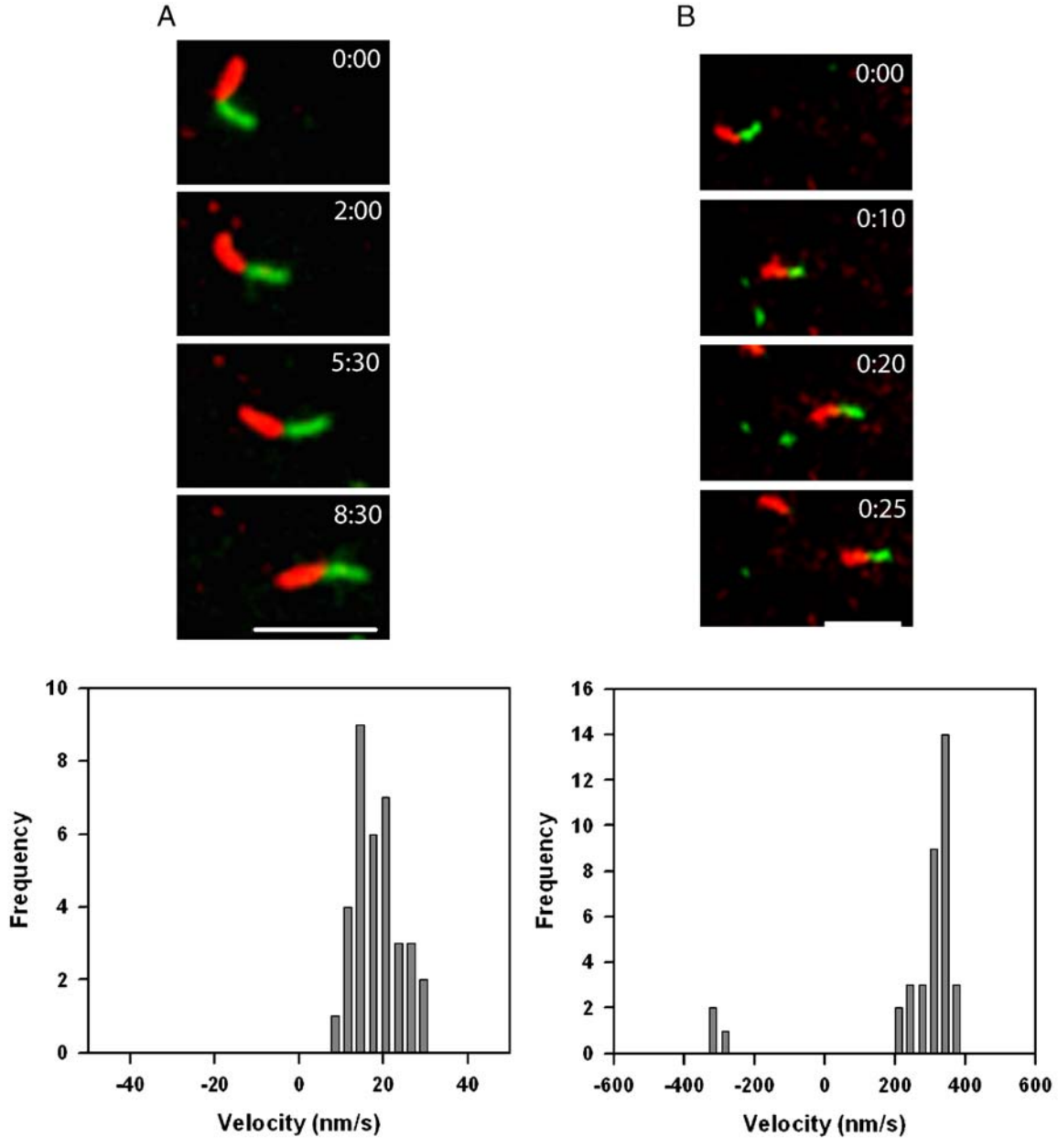

Fig. 5. Tail-less Myo9b is plus-end-directed. (A) A human Myo9b-CFP construct without most of the tail domain (amino acids 1–1201) was expressed in Cos cells and adsorbed onto a motility chamber with anti-GFP antibodies. Movement of polarity tagged actin filaments with Texas Red labeled plus ends was tracked by time-lapse microscopy (see Fig. 4C). Filament velocities were plotted as a histogram with plus-end-movement scored as a positive velocity and minus-end movement assigned a negative value. (B) The known plus-end-directed motor Myo5a was used as a control to assess the accuracy of the polarity tagged filaments in determining the direction of movement. The few apparent minus-end-directed filaments are likely due to polymerization off of the plus ends of plus-end seeds lacking gelsolin. Time shown is min:s. Scale bar, 5 μm.

indicating reversal of the lever arm is sufficient for reversing the direction of movement. Furthermore, the 2.9 Å resolution crystal structure of Myo6 in the post-power stroke state shows a striking reversal of the angle of the lever arm with respect to Myo5 [154]. The unique insertion and its CaM light chain interact with the converter domain and result in the emergence of the lever arm at a 120° angle relative to other myosins.

There is some evidence that under certain conditions in optical trap assays of single molecules, molecular motors can be induced to reverse their direction along the track. In general, motors will displace the bead from the center of the trap until a certain load, termed a stall force, is reached and then stop and detach. At high loads, Myo5a occasionally takes up to three steps in the reverse direction [105]. Backward steps were also observed when moderate loads (below stall force) were applied to Myo6 [97]. A more dramatic example of this behavior is exhibited by conventional kinesin when it is subjected to forces ~2× stall (17 pN). Under these conditions, processive backward stepping was observed, moving the bead back to the center of the trap until it reached stall force [155]. It is not clear how load reverses directionality. One possibility is that load physically pulls the lever arm so that it rotates in the opposite direction to unloaded conditions.

6. Conclusions

The motor properties of a myosin are defined by a combination of its enzyme kinetics and structural characteristics. Through extensive characterization of motors with biochemical and biophysical techniques it has become apparent that mechanochemistry is finely tuned to support the function of a given myosin. There also appear to be multiple mechanisms for accomplishing the same function. For example, long-range transport of cargo can take place utilizing a single molecule of a highly processive motor, such as vertebrate Myo5a, or with multiple non-processive motors such as Myo10. Also emerging is the extensive role of applied forces, such as backward or forward strain, in regulating the biochemical transitions, and therefore motor function, of an increasing large number of myosins. It is likely that myosins may function as cellular "tensiometers", providing a direct mechanism for transducing strain-mediated excellular cues to the cell interior. Undoubtedly, as more members of the myosin family are characterized, there will be additional and surprising mechanochemical adaptations uncovered.

Acknowledgements

This work was supported by NIH grants DK 25387 and GM 073823 (MSM).

References

[1] J.S. Berg, B.C. Powell, R.E. Cheney, A millennial myosin census, Mol. Biol. Cell 12 (2001) 780–794.
[2] T.A. Richards, T. Cavalier-Smith, Myosin domain evolution and the primary divergence of eukaryotes, Nature 436 (2005) 1113–1118.
[3] M. Krendel, M.S. Mooseker, Myosins: tails (and Heads) of functional diversity, Physiology (Bethesda) 20 (2005) 239–251.
[4] E.D. Korn, Coevolution of head, neck, and tail domains of myosin heavy chains, Proc. Natl. Acad. Sci. U. S. A. 97 (2000) 12559–12564.
[5] T.Q. Uyeda, S.J. Kron, J.A. Spudich, Myosin step size. Estimation from slow sliding movement of actin over low densities of heavy meromyosin, J. Mol. Biol. 214 (1990) 699–710.
[6] S.L. Reck-Peterson, M.J. Tyska, P.J. Novick, M.S. Mooseker, The yeast class V myosins, Myo2p and Myo4p, are nonprocessive actin-based motors, J. Cell Biol. 153 (2001) 1121–1126.
[7] P.L. Post, M.J. Tyska, C.B. O'Connell, K. Johung, A. Hayward, M.S. Mooseker, Myosin-IXb is a single-headed and processive motor, J. Biol. Chem. 277 (2002) 11679–11683.
[8] D.E. Harris, D.M. Warshaw, Smooth and skeletal muscle myosin both exhibit low duty cycles at zero load in vitro, J. Biol. Chem. 268 (1993) 14764–14768.
[9] R.W. Lymn, E.W. Taylor, Mechanism of adenosine triphosphate hydrolysis by actomyosin, Biochemistry 10 (1971) 4617–4624.
[10] M. Kovacs, F. Wang, A. Hu, Y. Zhang, J.R. Sellers, Functional divergence of human cytoplasmic myosin II: kinetic characterization of the non-muscle IIA isoform, J. Biol. Chem. 278 (2003) 38132–38140.
[11] F. Wang, M. Kovacs, A. Hu, J. Limouze, E.V. Harvey, J.R. Sellers, Kinetic mechanism of non-muscle myosin IIB: functional adaptations for tension generation and maintenance, J. Biol. Chem. 278 (2003) 27439–27448.
[12] S.S. Rosenfeld, J. Xing, L.Q. Chen, H.L. Sweeney, Myosin IIb is unconventionally conventional, J. Biol. Chem. 278 (2003) 27449–27455.
[13] M.E. Brown, P.C. Bridgman, Retrograde flow rate is increased in growth cones from myosin IIB knockout mice, J. Cell. Sci. 116 (2003) 1087–1094.
[14] E.M. Ostap, T.D. Pollard, Biochemical kinetic characterization of the Acanthamoeba myosin-I ATPase, J. Cell Biol. 132 (1996) 1053–1060.
[15] J.D. Jontes, R.A. Milligan, T.D. Pollard, E.M. Ostap, Kinetic characterization of brush border myosin-I ATPase, Proc. Natl. Acad. Sci. U. S. A. 94 (1997) 14332–14337.
[16] M. El Mezgueldi, N. Tang, S.S. Rosenfeld, E.M. Ostap, The kinetic mechanism of Myo1e (human myosin-IC), J. Biol. Chem. 277 (2002) 21514–21521.
[17] M.A. Titus, The role of unconventional myosins in Dictyostelium endocytosis, J. Eukaryot. Microbiol. 47 (2000) 191–196.
[18] R.I. Tuxworth, M.A. Titus, Unconventional myosins: anchors in the membrane traffic relay, Traffic 1 (2000) 11–18.
[19] A.E. Engqvist-Goldstein, D.G. Drubin, Actin assembly and endocytosis: from yeast to mammals, Annu. Rev. Cell Dev. Biol. 19 (2003) 287–332.
[20] M.S. Mooseker, L.G. Tilney, Organization of an actin filament–membrane complex. Filament polarity and membrane attachment in the microvilli of intestinal epithelial cells, J. Cell Biol. 67 (1975) 725–743.
[21] E.M. Ostap, P. Maupin, S.K. Doberstein, I.C. Baines, E.D. Korn, T.D. Pollard, Dynamic localization of myosin-I to endocytic structures in Acanthamoeba, Cell Motil. Cytoskelet. 54 (2003) 29–40.
[22] M.J. Tyska, M.S. Mooseker, A role for myosin-1A in the localization of a brush border disaccharidase, J. Cell Biol. 165 (2004) 395–405.
[23] A. Bretscher, Microfilament structure and function in the cortical cytoskeleton, Annu. Rev. Cell Biol. 7 (1991) 337–374.
[24] M.S. Mooseker, R.E. Cheney, Unconventional myosins, Annu. Rev. Cell Dev. Biol. 11 (1995) 633–675.
[25] M.J. Tyska, A.T. Mackey, J.D. Huang, N.G. Copeland, N.A. Jenkins, M.S. Mooseker, Myosin-1a is critical for normal brush border structure and composition, Mol. Biol. Cell 16 (2005) 2443–2457.
[26] J.S. Berg, R.E. Cheney, Myosin-X is an unconventional myosin that undergoes intrafilopodial motility, Nat. Cell Biol. 4 (2002) 246–250.
[27] H. Zhang, J.S. Berg, Z. Li, Y. Wang, P. Lang, A.D. Sousa, A. Bhaskar, R.E. Cheney, S. Stromblad, Myosin-X provides a motor-based link between integrins and the cytoskeleton, Nat. Cell Biol. 6 (2004) 523–531.
[28] H. Tokuo, M. Ikebe, Myosin X transports Mena/VASP to the tip of filopodia, Biochem. Biophys. Res. Commun. 319 (2004) 214–220.
[29] D. Cox, J.S. Berg, M. Cammer, J.O. Chinegwundoh, B.M. Dale, R.E.

Cheney, S. Greenberg, Myosin X is a downstream effector of PI(3)K during phagocytosis, Nat. Cell Biol. 4 (2002) 469–477.
[30] M. Kovacs, F. Wang, J.R. Sellers, Mechanism of action of myosin X, a membrane-associated molecular motor, J. Biol. Chem. 280 (2005) 15071–15083.
[31] P.J. Knight, K. Thirumurugan, Y. Xu, F. Wang, A.P. Kalverda, W.F. Stafford III, J.R. Sellers, M. Peckham, The predicted coiled-coil domain of myosin 10 forms a novel elongated domain that lengthens the head, J. Biol. Chem. 280 (2005) 34702–34708.
[32] B. MacIver, A. McCormack, R. Slee, M. Bownes, Identification of an essential gene encoding a class-V unconventional myosin in *Drosophila melanogaster*, Eur. J. Biochem. 257 (1998) 529–537.
[33] N. Bonafe, J.R. Sellers, Molecular characterization of myosin V from *Drosophila melanogaster*, J. Muscle Res. Cell Motil. 19 (1998) 129–141.
[34] V. Mermall, N. Bonafe, L. Jones, J.R. Sellers, L. Cooley, M.S. Mooseker, *Drosophila* myosin V is required for larval development and spermatid individualization, Dev. Biol. 286 (2005) 238–255.
[35] J. Toth, M. Kovacs, F. Wang, L. Nyitray, J.R. Sellers, Myosin V from *Drosophila* reveals diversity of motor mechanisms within the myosin V family, J. Biol. Chem. 280 (2005) 30594–30603.
[36] B. Govindan, R. Bowser, P. Novick, The role of Myo2, a yeast class V myosin, in vesicular transport, J. Cell Biol. 128 (1995) 1055–1068.
[37] I.R. Boldogh, S.L. Ramcharan, H.C. Yang, L.A. Pon, A type V myosin (Myo2p) and a Rab-like G-protein (Ypt11p) are required for retention of newly inherited mitochondria in yeast cells during cell division, Mol. Biol. Cell 15 (2004) 3994–4002.
[38] K.L. Hill, N.L. Catlett, L.S. Weisman, Actin and myosin function in directed vacuole movement during cell division in *Saccharomyces cerevisiae*, J. Cell Biol. 135 (1996) 1535–1549.
[39] H. Yin, D. Pruyne, T.C. Huffaker, A. Bretscher, Myosin V orientates the mitotic spindle in yeast, Nature 406 (2000) 1013–1015.
[40] G.B. Gonsalvez, C.R. Urbinati, R.M. Long, RNA localization in yeast: moving towards a mechanism, Biol. Cell 97 (2005) 75–86.
[41] P. Estrada, J. Kim, J. Coleman, L. Walker, B. Dunn, P. Takizawa, P. Novick, S. Ferro-Novick, Myo4p and She3p are required for cortical ER inheritance in *Saccharomyces cerevisiae*, J. Cell Biol. 163 (2003) 1255–1266.
[42] S.L. Reck-Peterson, D.W. Provance Jr., M.S. Mooseker, J.A. Mercer, Class V myosins, Biochim. Biophys. Acta 1496 (2000) 36–51.
[43] E.M. De La Cruz, A.L. Wells, S.S. Rosenfeld, E.M. Ostap, H.L. Sweeney, The kinetic mechanism of myosin V, Proc. Natl. Acad. Sci. U. S. A. 96 (1999) 13726–13731.
[44] R.E. Cheney, M.K. O'Shea, J.E. Heuser, M.V. Coelho, J.S. Wolenski, E.M. Espreafico, P. Forscher, R.E. Larson, M.S. Mooseker, Brain myosin-V is a two-headed unconventional myosin with motor activity, Cell 75 (1993) 13–23.
[45] A.A. Nascimento, R.E. Cheney, S.B. Tauhata, R.E. Larson, M.S. Mooseker, Enzymatic characterization and functional domain mapping of brain myosin-V, J. Biol. Chem. 271 (1996) 17561–17569.
[46] S.B. Tauhata, D.V. dos Santos, E.W. Taylor, M.S. Mooseker, R.E. Larson, High affinity binding of brain myosin-Va to F-actin induced by calcium in the presence of ATP, J. Biol. Chem. 276 (2001) 39812–39818.
[47] A.D. Mehta, R.S. Rock, M. Rief, J.A. Spudich, M.S. Mooseker, R.E. Cheney, Myosin-V is a processive actin-based motor, Nature 400 (1999) 590–593.
[48] R.S. Rock, M. Rief, A.D. Mehta, J.A. Spudich, In vitro assays of processive myosin motors, Methods 22 (2000) 373–381.
[49] C. Veigel, S. Schmitz, F. Wang, J.R. Sellers, Load-dependent kinetics of myosin-V can explain its high processivity, Nat. Cell Biol. 7 (2005) 861–869.
[50] T.J. Purcell, H.L. Sweeney, J.A. Spudich, A force-dependent state controls the coordination of processive myosin V, Proc. Natl. Acad. Sci. U. S. A. 102 (2005) 13873–13878.
[51] I. Rayment, W.R. Rypniewski, K. Schmidt-Base, R. Smith, D.R. Tomchick, M.M. Benning, D.A. Winkelmann, G. Wesenberg, H.M. Holden, Three-dimensional structure of myosin subfragment-1: a molecular motor, Science 261 (1993) 50–58.
[52] M. Furch, M.A. Geeves, D.J. Manstein, Modulation of actin affinity and actomyosin adenosine triphosphatase by charge changes in the myosin motor domain, Biochemistry 37 (1998) 6317–6326.
[53] C.T. Murphy, J.A. Spudich, The sequence of the myosin 50-20 K loop affects myosin's affinity for actin throughout the actin–myosin ATPase cycle and its maximum ATPase activity, Biochemistry 38 (1999) 3785–3792.
[54] P.B. Joel, H.L. Sweeney, K.M. Trybus, Addition of lysines to the 50/20 kDa junction of myosin strengthens weak binding to actin without affecting the maximum ATPase activity, Biochemistry 42 (2003) 9160–9166.
[55] C.M. Yengo, H.L. Sweeney, Functional role of loop 2 in myosin V, Biochemistry 43 (2004) 2605–2612.
[56] N. Volkmann, H. Liu, L. Hazelwood, E.B. Krementsova, S. Lowey, K.M. Trybus, D. Hanein, The structural basis of myosin V processive movement as revealed by electron cryomicroscopy, Mol. Cell 19 (2005) 595–605.
[57] K.A. Kellerman, K.G. Miller, An unconventional myosin heavy chain gene from *Drosophila melanogaster*, J. Cell Biol. 119 (1992) 823–834.
[58] E.R. Geisbrecht, D.J. Montell, Myosin VI is required for E-cadherin-mediated border cell migration, Nat. Cell Biol. 4 (2002) 616–620.
[59] H. Yoshida, W. Cheng, J. Hung, D. Montell, E. Geisbrecht, D. Rosen, J. Liu, H. Naora, Lessons from border cell migration in the *Drosophila* ovary: a role for myosin VI in dissemination of human ovarian cancer, Proc. Natl. Acad. Sci. U. S. A. (2004).
[60] F. Buss, S.D. Arden, M. Lindsay, J.P. Luzio, J. Kendrick-Jones, Myosin VI isoform localized to clathrin-coated vesicles with a role in clathrin-mediated endocytosis, EMBO J. 20 (2001) 3676–3684.
[61] L. Aschenbrenner, T. Lee, T. Hasson, Myo6 facilitates the translocation of endocytic vesicles from cell peripheries, Mol. Biol. Cell 14 (2003) 2728–2743.
[62] L. Aschenbrenner, S.N. Naccache, T. Hasson, Uncoated endocytic vesicles require the unconventional myosin, Myo6, for rapid transport through actin barriers, Mol. Biol. Cell 15 (2004) 2253–2263.
[63] C.L. Warner, A. Stewart, J.P. Luzio, K.P. Steel, R.T. Libby, J. Kendrick-Jones, F. Buss, Loss of myosin VI reduces secretion and the size of the Golgi in fibroblasts from Snell's waltzer mice, EMBO J. 22 (2003) 569–579.
[64] D.A. Sahlender, R.C. Roberts, S.D. Arden, G. Spudich, M.J. Taylor, J.P. Luzio, J. Kendrick-Jones, F. Buss, Optineurin links myosin VI to the Golgi complex and is involved in Golgi organization and exocytosis, J. Cell Biol. 169 (2005) 285–295.
[65] K.B. Avraham, T. Hasson, K.P. Steel, D.M. Kingsley, L.B. Russell, M.S. Mooseker, N.G. Copeland, N.A. Jenkins, The mouse Snell's waltzer deafness gene encodes an unconventional myosin required for structural integrity of inner ear hair cells, Nat. Genet. 11 (1995) 369–375.
[66] J.A. Kappler, C.J. Starr, D.K. Chan, R. Kollmar, A.J. Hudspeth, A nonsense mutation in the gene encoding a zebrafish myosin VI isoform causes defects in hair-cell mechanotransduction, Proc. Natl. Acad. Sci. U. S. A. 101 (2004) 13056–13061.
[67] S. Melchionda, N. Ahituv, L. Bisceglia, T. Sobe, F. Glaser, R. Rabionet, M.L. Arbones, A. Notarangelo, E. Di Iorio, M. Carella, L. Zelante, X. Estivill, K.B. Avraham, P. Gasparini, MYO6, the human homologue of the gene responsible for deafness in Snell's waltzer mice, is mutated in autosomal dominant nonsyndromic hearing loss, Am. J. Hum. Genet. 69 (2001) 635–640.
[68] C. Seiler, O. Ben-David, S. Sidi, O. Hendrich, A. Rusch, B. Burnside, K.B. Avraham, T. Nicolson, Myosin VI is required for structural integrity of the apical surface of sensory hair cells in zebrafish, Dev. Biol. 272 (2004) 328–338.
[69] S.A. Mohiddin, Z.M. Ahmed, A.J. Griffith, D. Tripodi, T.B. Friedman, L. Fananapazir, R.J. Morell, Novel association of hypertrophic cardiomyopathy, sensorineural deafness, and a mutation in unconventional myosin VI (MYO6), J. Med. Genet. 41 (2004) 309–314.
[70] E.M. De La Cruz, E.M. Ostap, H.L. Sweeney, Kinetic mechanism and regulation of myosin VI, J. Biol. Chem. 276 (2001) 32373–32381.
[71] M. Yoshimura, K. Homma, J. Saito, A. Inoue, R. Ikebe, M. Ikebe, Dual regulation of mammalian myosin VI motor function, J. Biol. Chem. 276 (2001) 39600–39607.

[72] I. Lister, S. Schmitz, M. Walker, J. Trinick, F. Buss, C. Veigel, J. Kendrick-Jones, A monomeric myosin VI with a large working stroke, EMBO J. 23 (2004) 1729–1738.
[73] R.T. Libby, K.P. Steel, The roles of unconventional myosins in hearing and deafness, Essays Biochem. 35 (2000) 159–174.
[74] M.J. Redowicz, Myosins and pathology: genetics and biology, Acta Biochim. Pol. 49 (2002) 789–804.
[75] L.E. Soni, C.M. Warren, C. Bucci, D.J. Orten, T. Hasson, The unconventional myosin-VIIa associates with lysosomes, Cell Motil. Cytoskelet. 62 (2005) 13–26.
[76] S. Watanabe, R. Ikebe, M. Ikebe, *Drosophila* myosin VIIA is a high duty ratio motor with a unique kinetic mechanism, J. Biol. Chem. 281 (2006) 7151–7160.
[77] D. Weil, G. Levy, I. Sahly, F. Levi-Acobas, S. Blanchard, A. El-Amraoui, F. Crozet, H. Philippe, M. Abitbol, C. Petit, Human myosin VIIA responsible for the Usher 1B syndrome: a predicted membrane-associated motor protein expressed in developing sensory epithelia, Proc. Natl. Acad. Sci. U. S. A. 93 (1996) 3232–3237.
[78] A. Inoue, M. Ikebe, Characterization of the motor activity of mammalian myosin VIIA, J. Biol. Chem. 278 (2003) 5478–5487.
[79] Z.Y. Chen, T. Hasson, D.S. Zhang, B.J. Schwender, B.H. Derfler, M.S. Mooseker, D.P. Corey, Myosin-VIIb, a novel unconventional myosin, is a constituent of microvilli in transporting epithelia, Genomics 72 (2001) 285–296.
[80] A. Henn, E.M. De La Cruz, Vertebrate myosin VIIb is a high duty ratio motor adapted for generating and maintaining tension, J. Biol. Chem. 280 (2005) 39665–39676.
[81] Y. Yang, M. Kovacs, Q. Xu, J.B. Anderson, J.R. Sellers, Myosin VIIB from *Drosophila* is a high duty ratio motor, J. Biol. Chem. 280 (2005) 32061–32068.
[82] S. Higashi-Fujime, R. Ishikawa, H. Iwasawa, O. Kagami, E. Kurimoto, K. Kohama, T. Hozumi, The fastest actin-based motor protein from the green algae, Chara, and its distinct mode of interaction with actin, FEBS Lett. 375 (1995) 151–154.
[83] Z. Wang, T.C. Pesacreta, A subclass of myosin XI is associated with mitochondria, plastids, and the molecular chaperone subunit TCP-1alpha in maize, Cell Motil. Cytoskelet. 57 (2004) 218–232.
[84] K. Hashimoto, H. Igarashi, S. Mano, M. Nishimura, T. Shimmen, E. Yokota, Peroxisomal localization of a myosin XI isoform in *Arabidopsis thaliana*, Plant Cell Physiol. 46 (2005) 782–789.
[85] M. Morimatsu, A. Nakamura, H. Sumiyoshi, N. Sakaba, H. Taniguchi, K. Kohama, S. Higashi-Fujime, The molecular structure of the fastest myosin from green algae, Chara, Biochem. Biophys. Res. Commun. 270 (2000) 147–152.
[86] M. Tominaga, H. Kojima, E. Yokota, H. Orii, R. Nakamori, E. Katayama, M. Anson, T. Shimmen, K. Oiwa, Higher plant myosin XI moves processively on actin with 35 nm steps at high velocity, EMBO J. 22 (2003) 1263–1272.
[87] R.T. Muller, U. Honnert, J. Reinhard, M. Bahler, The rat myosin myr 5 is a GTPase-activating protein for Rho in vivo: essential role of arginine 1695, Mol. Biol. Cell 8 (1997) 2039–2053.
[88] J. Reinhard, A.A. Scheel, D. Diekmann, A. Hall, C. Ruppert, M. Bahler, A novel type of myosin implicated in signalling by rho family GTPases, EMBO J. 14 (1995) 697–704.
[89] J.A. Wirth, K.A. Jensen, P.L. Post, W.M. Bement, M.S. Mooseker, Human myosin-IXb, an unconventional myosin with a chimerin-like rho/rac GTPase-activating protein domain in its tail, J. Cell Sci. 109 (Pt. 3) (1996) 653–661.
[90] P.L. Post, G.M. Bokoch, M.S. Mooseker, Human myosin-IXb is a mechanochemically active motor and a GAP for rho, 111 (1998) 941–950.
[91] A. Inoue, J. Saito, R. Ikebe, M. Ikebe, Myosin IXb is a single-headed minus-end-directed processive motor, Nat. Cell Biol. 4 (2002) 302–306.
[92] V. Nalavadi, M. Nyitrai, C. Bertolini, N. Adamek, M. Geeves, M. Bahler, Kinetic mechanism of myosin IXB and the contributions of two class lX specific regions, J. Biol. Chem. (2005).
[93] T. Kambara, M. Ikebe, A unique ATP hydrolysis mechanism of single-headed processive myosin, myosin IX, J. Biol. Chem. (2005).
[94] Y. Okada, N. Hirokawa, Mechanism of the single-headed processivity: diffusional anchoring between the K-loop of kinesin and the C terminus of tubulin, Proc. Natl. Acad. Sci. U. S. A. 97 (2000) 640–645.
[95] J.E. Baker, E.B. Krementsova, G.G. Kennedy, A. Armstrong, K.M. Trybus, D.M. Warshaw, Myosin V processivity: multiple kinetic pathways for head-to-head coordination, Proc. Natl. Acad. Sci. U. S. A. 101 (2004) 5542–5546.
[96] T. Sakamoto, I. Amitani, E. Yokota, T. Ando, Direct observation of processive movement by individual myosin V molecules, Biochem. Biophys. Res. Commun. 272 (2000) 586–590.
[97] R.S. Rock, S.E. Rice, A.L. Wells, T.J. Purcell, J.A. Spudich, H.L. Sweeney, Myosin VI is a processive motor with a large step size, Proc. Natl. Acad. Sci. U. S. A. 98 (2001) 13655–13659.
[98] S. Nishikawa, K. Homma, Y. Komori, M. Iwaki, T. Wazawa, A. Hikikoshi Iwane, J. Saito, R. Ikebe, E. Katayama, T. Yanagida, M. Ikebe, Class VI myosin moves processively along actin filaments backward with large steps, Biochem. Biophys. Res. Commun. 290 (2002) 311–317.
[99] W.O. Hancock, J. Howard, Processivity of the motor protein kinesin requires two heads, J. Cell Biol. 140 (1998) 1395–1405.
[100] H. Sakakibara, H. Kojima, Y. Sakai, E. Katayama, K. Oiwa, Inner-arm dynein c of Chlamydomonas flagella is a single-headed processive motor, Nature 400 (1999) 586–590.
[101] M.J. Tyska, D.M. Warshaw, The myosin power stroke, Cell Motil. Cytoskelet. 51 (2002) 1–15.
[102] J.T. Finer, R.M. Simmons, J.A. Spudich, Single myosin molecule mechanics: piconewton forces and nanometre steps, Nature 368 (1994) 113–119.
[103] C. Veigel, L.M. Coluccio, J.D. Jontes, J.C. Sparrow, R.A. Milligan, J.E. Molloy, The motor protein myosin-I produces its working stroke in two steps, Nature 398 (1999) 530–533.
[104] K. Homma, J. Saito, R. Ikebe, M. Ikebe, Motor function and regulation of myosin X, J. Biol. Chem. 276 (2001) 34348–34354.
[105] A.D. Mehta, R.S. Rock, M. Rief, S.A. Spudich, M.S. Mooseker, R.E. Cheney, Myosin-V is a processive actin-based motor, Nature 400 (1999) 590–593.
[106] E.B. Krementsova, A.R. Hodges, H. Lu, K.M. Trybus, Processivity of chimeric class V myosins, J. Biol. Chem. 281 (2006) 6079–6086.
[107] M. Iwaki, H. Tanaka, A.H. Iwane, E. Katayama, M. Ikebe, T. Yanagida, Cargo binding makes a wild-type single-headed myosin-VI move processively, Biophys. J. (2006).
[108] H. Park, B. Ramamurthy, M. Travaglia, D. Safer, L.Q. Chen, C. Franzini-Armstrong, P.R. Selvin, H.L. Sweeney, Full-length myosin VI dimerizes and moves processively along actin filaments upon monomer clustering, Mol. Cell 21 (2006) 331–336.
[109] F. Buss, G. Spudich, J. Kendrick-Jones, Myosin VI: cellular functions and motor properties, Annu. Rev. Cell Dev. Biol. 20 (2004) 649–676.
[110] T. Hasson, Myosin VI: two distinct roles in endocytosis, J. Cell. Sci. 116 (2003) 3453–3461.
[111] M. Nishikawa, S. Nishikawa, A. Inoue, A.H. Iwane, T. Yanagida, M. Ikebe, A unique mechanism for the processive movement of single-headed myosin-IX, Biochem. Biophys. Res. Commun. 343 (2006) 1159–1164.
[112] H.E. Huxley, The mechanism of muscular contraction, Science 164 (1969) 1356–1365.
[113] A.J. Fisher, C.A. Smith, J.B. Thoden, R. Smith, K. Sutoh, H.M. Holden, I. Rayment, X-ray structures of the myosin motor domain of *Dictyostelium discoideum* complexed with MgADP, BeFx and MgADP.AlF4, Biochemistry 34 (1995) 8960–8972.
[114] C.A. Smith, I. Rayment, X-ray structure of the magnesium(II).ADP. vanadate complex of the *Dictyostelium discoideum* myosin motor domain to 1.9 A resolution, Biochemistry 35 (1996) 5404–5417.
[115] R. Dominguez, Y. Freyzon, K.M. Trybus, C. Cohen, Crystal structure of a vertebrate smooth muscle myosin motor domain and its complex with the essential light chain: visualization of the pre-power stroke state, Cell 94 (1998) 559–571.
[116] A. Houdusse, V.N. Kalabokis, D. Himmel, A.G. Szent-Gyorgyi, C. Cohen, Atomic structure of scallop myosin subfragment S1 complexed

with MgADP: a novel conformation of the myosin head, Cell 97 (1999) 459–470.
[117] A. Houdusse, A.G. Szent-Gyorgyi, C. Cohen, Three conformational states of scallop myosin S1, Proc. Natl. Acad. Sci. U. S. A. 97 (2000) 11238–11243.
[118] M.L. Walker, S.A. Burgess, J.R. Sellers, F. Wang, J.A. Hammer III, J. Trinick, P.J. Knight, Two-headed binding of a processive myosin to F-actin, Nature 405 (2000) 804–807.
[119] T.J. Purcell, C. Morris, J.A. Spudich, H.L. Sweeney, Role of the lever arm in the processive stepping of myosin V, Proc. Natl. Acad. Sci. U. S. A. 99 (2002) 14159–14164.
[120] T. Sakamoto, F. Wang, S. Schmitz, Y. Xu, Q. Xu, J.E. Molloy, C. Veigel, J.R. Sellers, Neck length and processivity of myosin V, J. Biol. Chem. 278 (2003) 29201–29207.
[121] W. Hua, J. Chung, J. Gelles, Distinguishing inchworm and hand-over-hand processive kinesin movement by neck rotation measurements, Science 295 (2002) 844–848.
[122] T. Yanagida, K. Kitamura, H. Tanaka, A. Hikikoshi Iwane, S. Esaki, Single molecule analysis of the actomyosin motor, Curr. Opin. Cell Biol. 12 (2000) 20–25.
[123] J.N. Forkey, M.E. Quinlan, M.A. Shaw, J.E. Corrie, Y.E. Goldman, Three-dimensional structural dynamics of myosin V by single-molecule fluorescence polarization, Nature 422 (2003) 399–404.
[124] A. Yildiz, J.N. Forkey, S.A. McKinney, T. Ha, Y.E. Goldman, P.R. Selvin, Myosin V walks hand-over-hand: single fluorophore imaging with 1.5-nm localization, Science 300 (2003) 2061–2065.
[125] D.M. Warshaw, G.G. Kennedy, S.S. Work, E.B. Krementsova, S. Beck, K.M. Trybus, Differential labeling of myosin V heads with quantum dots allows direct visualization of hand-over-hand processivity, Biophys. J. 88 (2005) L30–L32.
[126] A. Mehta, Myosin learns to walk, J. Cell. Sci. 114 (2001) 1981–1998.
[127] A. Yildiz, H. Park, D. Safer, Z. Yang, L.Q. Chen, P.R. Selvin, H.L. Sweeney, Myosin VI steps via a hand-over-hand mechanism with its lever arm undergoing fluctuations when attached to actin, J. Biol. Chem. 279 (2004) 37223–37226.
[128] Z. Okten, L.S. Churchman, R.S. Rock, J.A. Spudich, Myosin VI walks hand-over-hand along actin, Nat. Struct. Mol. Biol. 11 (2004) 884–887.
[129] A. Bahloul, G. Chevreux, A.L. Wells, D. Martin, J. Nolt, Z. Yang, L.Q. Chen, N. Potier, A. Van Dorsselaer, S. Rosenfeld, A. Houdusse, H.L. Sweeney, The unique insert in myosin VI is a structural calcium-calmodulin binding site, Proc. Natl. Acad. Sci. U. S. A. 101 (2004) 4787–4792.
[130] H. Balci, T. Ha, H.L. Sweeney, P.R. Selvin, Interhead distance measurements in myosin VI via SHRImP support a simplified hand-over-hand model, Biophys. J. 89 (2005) 413–417.
[131] D. Altman, H.L. Sweeney, J.A. Spudich, The mechanism of myosin VI translocation and its load-induced anchoring, Cell 116 (2004) 737–749.
[132] R.S. Rock, B. Ramamurthy, A.R. Dunn, S. Beccafico, B.R. Rami, C. Morris, B.J. Spink, C. Franzini-Armstrong, J.A. Spudich, H.L. Sweeney, A flexible domain is essential for the large step size and processivity of myosin VI, Mol. Cell 17 (2005) 603–609.
[133] R.A. Kammerer, T. Schulthess, R. Landwehr, A. Lustig, J. Engel, U. Aebi, M.O. Steinmetz, An autonomous folding unit mediates the assembly of two-stranded coiled coils, Proc. Natl. Acad. Sci. U. S. A. 95 (1998) 13419–13424.
[134] J.D. Jontes, E.M. Wilson-Kubalek, R.A. Milligan, A 32 degree tail swing in brush border myosin I on ADP release, Nature 378 (1995) 751–753.
[135] C. Veigel, J.E. Molloy, S. Schmitz, J. Kendrick-Jones, Load-dependent kinetics of force production by smooth muscle myosin measured with optical tweezers, Nat. Cell Biol. 5 (2003) 980–986.
[136] C. Veigel, F. Wang, M.L. Bartoo, J.R. Sellers, J.E. Molloy, The gated gait of the processive molecular motor, myosin V, Nat. Cell Biol. 4 (2002) 59–65.
[137] J.S. Wolenski, S.M. Hayden, P. Forscher, M.S. Mooseker, Calcium-calmodulin and regulation of brush border myosin-I MgATPase and mechanochemistry, 122 (1993) 613–621.
[138] K. Collins, J.R. Sellers, P. Matsudaira, Calmodulin dissociation regulates brush border myosin I (110-kD-calmodulin) mechanochemical activity in vitro, J. Cell Biol. 110 (1990) 1137–1147.
[139] S.J. Kron, J.A. Spudich, Fluorescent actin filaments move on myosin fixed to a glass surface, Proc. Natl. Acad. Sci. U. S. A. 83 (1986) 6272–6276.
[140] J.S. Wolenski, R.E. Cheney, P. Forscher, M.S. Mooseker, In vitro motilities of the unconventional myosins, brush border myosin-I, and chick brain myosin-V exhibit assay-dependent differences in velocity, J. Exp. Zool. 267 (1993) 33–39.
[141] J.S. Wolenski, R.E. Cheney, M.S. Mooseker, P. Forscher, In vitro motility of immunoadsorbed brain myosin-V using a Limulus acrosomal process and optical tweezer-based assay, J. Cell. Sci. 108 (Pt. 4) (1995) 1489–1496.
[142] A.L. Wells, A.W. Lin, L.Q. Chen, D. Safer, S.M. Cain, T. Hasson, B.O. Carragher, R.A. Milligan, H.L. Sweeney, Myosin VI is an actin-based motor that moves backwards, Nature 401 (1999) 505–508.
[143] C.A. Morris, A.L. Wells, Z. Yang, L.Q. Chen, C.V. Baldacchino, H.L. Sweeney, Calcium functionally uncouples the heads of myosin VI, J. Biol. Chem. 278 (2003) 23324–23330.
[144] T. Self, T. Sobe, N.G. Copeland, N.A. Jenkins, K.B. Avraham, K.P. Steel, Role of myosin VI in the differentiation of cochlear hair cells, Dev. Biol. 214 (1999) 331–341.
[145] T. Hasson, P.G. Gillespie, J.A. Garcia, R.B. MacDonald, Y. Zhao, A.G. Yee, M.S. Mooseker, D.P. Corey, Unconventional myosins in inner-ear sensory epithelia, J. Cell Biol. 137 (1997) 1287–1307.
[146] M.P. Sheetz, J.A. Spudich, Movement of myosin-coated structures on actin cables, Cell Motil. 3 (1983) 485–489.
[147] M.P. Sheetz, J.A. Spudich, Movement of myosin-coated fluorescent beads on actin cables in vitro, Nature 303 (1983) 31–35.
[148] L.G. Tilney, Actin filaments in the acrosomal reaction of Limulus sperm. Motion generated by alterations in the packing of the filaments, J. Cell Biol. 64 (1975) 289–310.
[149] M.F. Schmid, P. Matsudaira, T.W. Jeng, J. Jakana, E. Towns-Andrews, J. Bordas, W. Chiu, Crystallographic analysis of acrosomal bundle from Limulus sperm, J. Mol. Biol. 221 (1991) 711–725.
[150] A. Herm-Gotz, S. Weiss, R. Stratmann, S. Fujita-Becker, C. Ruff, E. Meyhofer, T. Soldati, D.J. Manstein, M.A. Geeves, D. Soldati, *Toxoplasma gondii* myosin A and its light chain: a fast, single-headed, plus-end-directed motor, EMBO J. 21 (2002) 2149–2158.
[151] C.B. O'Connell, M.S. Mooseker, Native myosin-IXb is a plus-, not a minus-end-directed motor, Nat. Cell Biol. 5 (2003) 171–172.
[152] K. Homma, M. Yoshimura, J. Saito, R. Ikebe, M. Ikebe, The core of the motor domain determines the direction of myosin movement, Nature 412 (2001) 831–834.
[153] G. Tsiavaliaris, S. Fujita-Becker, D.J. Manstein, Molecular engineering of a backwards-moving myosin motor, Nature 427 (2004) 558–561.
[154] J. Menetrey, A. Bahloul, A.L. Wells, C.M. Yengo, C.A. Morris, H.L. Sweeney, A. Houdusse, The structure of the myosin VI motor reveals the mechanism of directionality reversal, Nature 435 (2005) 779–785.
[155] N.J. Carter, R.A. Cross, Mechanics of the kinesin step, Nature 435 (2005) 308–312.
[156] M.S. Mooseker, T.R. Coleman, The 110-kD protein–calmodulin complex of the intestinal microvillus (brush border myosin I) is a mechanoenzyme, J. Cell Biol. 108 (1989) 2395–2400.
[157] T. Lin, N. Tang, E.M. Ostap, Biochemical and motile properties of Myo1b splice isoforms, J. Biol. Chem. 280 (2005) 41562–41567.
[158] D.M. Warshaw, J.M. Desrosiers, S.S. Work, K.M. Trybus, Smooth muscle myosin cross-bridge interactions modulate actin filament sliding velocity in vitro, J. Cell Biol. 111 (1990) 453–463.
[159] F. Wang, E.V. Harvey, M.A. Conti, D. Wei, J.R. Sellers, A conserved negatively charged amino acid modulates function in human nonmuscle myosin IIA, Biochemistry 39 (2000) 5555–5560.
[160] M.D. Pato, J.R. Sellers, Y.A. Preston, E.V. Harvey, R.S. Adelstein, Baculovirus expression of chicken nonmuscle heavy meromyosin II-B. Characterization of alternatively spliced isoforms, J. Biol. Chem. 271 (1996) 2689–2695.

[161] S. Komaba, A. Inoue, S. Maruta, H. Hosoya, M. Ikebe, Determination of human myosin III as a motor protein having a protein kinase activity, J. Biol. Chem. 278 (2003) 21352–21360.
[162] E.B. Krementsova, A.R. Hodges, H. Lu, K.M. Trybus, Processivity of chimeric class V myosins, J. Biol. Chem. (2005).
[163] S. Watanabe, K. Mabuchi, R. Ikebe, M. Ikebe, Mechanoenzymatic characterization of human Myosin vb, Biochemistry 45 (2006) 2729–2738.
[164] I.P. Udovichenko, D. Gibbs, D.S. Williams, Actin-based motor properties of native myosin VIIa, J. Cell. Sci. 115 (2002) 445–450.
[165] K. Homma, M. Ikebe, Myosin X is a high duty ratio motor, J. Biol. Chem. 280 (2005) 29381–29391.